Gaussian Models for Observed Dispersion in High Redshift Gamma Ray Bursts

Thomas P. Weldon, Ryan S. Adams, and Kasra Daneshvar
Department of Electrical and Computer Engineering
University of North Carolina at Charlotte
Charlotte, NC 28223, USA
Email: tpweldon@uncc.edu

***Abstract*—Astronomical observations of gamma-ray bursts commonly exhibit dispersive behavior where high-energy gamma rays arrive significantly later than low-energy photons. Although certain quantum gravity theories suggest such dispersion, the underlying mechanisms are not yet fully understood. Nevertheless, a quadratic polynomial model has been proposed for the frequency-dependent photon velocity. Substituting this model into the Helmholtz equation then leads to a number of candidate forms of the underlying differential equations, where additional terms in the Maxwell equations model the observed dispersion. Unfortunately, this quadratic dispersion model results in unusual behavior such as superluminal velocity. Therefore, a new Gaussian dispersion model is also proposed. This Gaussian model closely approximates the quadratic model at low frequencies while avoiding the superluminal behavior of quadratic models.**

I. Introduction

Since its launch in 2008, the Fermi Gamma-ray Space Telescope has enhanced the ability to measure dispersion of high-energy photons in gamma-ray bursts [1]. Although such dispersive effects are predicted by certain quantum gravity models, the mechanisms underlying the observed dispersion remain uncertain. Nevertheless, a quadratic polynomial model has been proposed for the measured frequency-dependent velocity of high-energy photons [2], [3]. While a linear dispersion model appears unlikely based on data from gamma-ray burst GRB 090510 in May of 2009, quadratic dispersion models have not yet been disproven [4]. In this gamma-ray burst, photons at 31 GeV (7.5×10^{24} Hz) arrived as much as hundreds of milliseconds later than low energy photons. Such dispersive phenomena may be predicted by quadratic quantum gravity models at extremely high frequencies, where photon energies approach the Planck scale of 1.22×10^{19} GeV [4].

Since linear dispersion models appear unlikely, the remainder of the paper focuses on quadratic models and corresponding candidate forms of the underlying differential equations. In the following, the quadratic dispersion models are first substituted into the Helmholtz equation. This modified Helmholtz equation, in turn, suggests possible forms for the underlying differential equations. The resulting candidates resemble Maxwell's equations, with additional terms accounting for dispersion. Interestingly, the primary candidate resembles a dual composite right/left-handed (D-CRLH) metamaterial model [5]. This similarity to metamaterials provides useful insight into the behavior of the model, such as left-handed propagation and superluminal velocity. The present work offers a novel alternative Gaussian dispersion model that does not exhibit the superluminal behavior associated with the quadratic model. In addition, the present work compares measured dispersive time delays with predicted time delays, including adjustment of the predicted time delay for observed redshift and cosmological distances.

In the following development, dispersive propagation models are formulated directly from the measured dispersion data of gamma-ray bursts. In essence, the approach is to fit a simple polynomial model to the measured data. This empirical approach therefore avoids controversial quantum gravity arguments and the need for theoretical details of the physical mechanisms of the dispersion. The corresponding differential equations that follow from the development result in additional terms in Maxwell's equations that model the observed dispersion. Finally, a novel Gaussian dispersion model is proposed as an alternative model that does not exhibit the superliminal behavior associated with a quadratic model.

II. Empirical Quadratic Dispersion Model

In previous investigations of dispersion in gamma-ray bursts, the velocity of light has been modeled as a power series expansion for high photon energies [2], [3]. In these models, the photon group velocity v_g is typically expressed as a function of photon energy $\mathcal{E}_\omega$, or of angular frequency ω, up to second order [2], [5]

$$v_g \approx c\left(1 - \xi\frac{\mathcal{E}_\omega}{\mathcal{E}_p} - \zeta\frac{{\mathcal{E}_\omega}^2}{\mathcal{E}_p^2}\right) = c\left(1 - a_1\omega - a_2\omega^2\right), \qquad (1)$$

where $\mathcal{E}_\omega = h\omega/(2\pi)$ is photon energy in eV, ω is photon frequency in rad/s, Planck's constant is $h = 4.14\times10^{-15}$ eV·s, $\mathcal{E}_p = 1.22 \times 10^{28}$ eV is the Planck energy, $c = 3.0\times10^{8}$ m/s, and ξ, ζ, $a_1 = \xi h/(2\pi\mathcal{E}_p)$, and $a_2 = \zeta h^2/(2\pi\mathcal{E}_p)^2$ are free parameters [2].

However, recent measured data from gamma-ray burst GRB 090510 suggests that the linear term in (1) may be zero [4]. In this case, let $a_1 = 0$, and the model for photon group velocity v_g and phase velocity v_p may be further simplified as

$$v_g \approx c\left(1 - a_2\omega^2\right) \text{ and } v_p \approx c\left(1 - a_2\omega^2/3\right). \qquad (2)$$

where v_g is consistent with v_p, since $v_p = \omega/k$ gives $k = \omega/(c - a_2\omega^2 c/3) \approx \omega(1 + a_2\omega^2/3)/c = (\omega + a_2\omega^3/3)/c$ for

$a_2\omega^2/3 \ll 1$. Then, $\partial k/\partial\omega = (1+a_2\omega^2)/c$, and so $v_g = \partial\omega/\partial k = c/(1+a_2\omega^2) \approx c(1-a_2\omega^2)$ as given in (2).

The above dispersion relation (2) is next substituted into the Helmholtz equation. To begin, consider the Helmholtz equation in vacuum for low energy photons [6]

$$\nabla^2\mathbf{E} = \frac{-\omega^2}{c^2}\mathbf{E} = -\omega^2\mu_\circ\epsilon_\circ\mathbf{E}, \tag{3}$$

and the corresponding free-space form of Maxwell's equations

$$\begin{aligned} \nabla\times\mathbf{E} &= -j\omega\mu_\circ\mathbf{H} \\ \nabla\times\mathbf{H} &= j\omega\epsilon_\circ\mathbf{E}, \end{aligned} \tag{4}$$

where the permittivity of free space is $\epsilon_\circ = 8.85\times10^{-12}$ F/m and the permeability of free space is $\mu_\circ = 1.26\times10^{-6}$ H/m. Substituting the dispersive velocity v_p from (2) for the constant velocity c in (3) gives the proposed dispersive form of the Helmholtz equation

$$\begin{aligned} \nabla^2\mathbf{E} &= \frac{-\omega^2}{c^2\left(1-a_2\omega^2/3\right)^2}\mathbf{E} \\ &= -\frac{\mu_\circ}{(1-a_2\omega^2/3)}\frac{\epsilon_\circ}{(1-a_2\omega^2/3)}\omega^2\mathbf{E}, \end{aligned} \tag{5}$$

where, for present purposes, the denominator terms beneath ϵ_0 and μ_0 were equally distributed on the right side of (5). Equation (5) would then have the plane-wave solution

$$\mathbf{E} = \mathbf{E}_\circ e^{-jkx}e^{j\omega t} = \mathbf{E}_\circ e^{-j\omega x/v_p}e^{j\omega t}, \tag{6}$$

where the the wavenumber is $k = \omega/v_p$. Comparison of (5) with (3) further suggests that Maxwell's equations in (4) should then become:

$$\begin{aligned} \nabla\times\mathbf{E} &= -\frac{j\omega\mu_\circ}{(1-a_2\omega^2/3)}\mathbf{H} \\ \nabla\times\mathbf{H} &= \frac{j\omega\epsilon_\circ}{(1-a_2\omega^2/3)}\mathbf{E}, \end{aligned} \tag{7}$$

or:

$$\begin{aligned} \nabla\times\mathbf{E} - a_2\omega^2\left(\nabla\times\mathbf{E}\right)/3 &= -j\omega\mu_\circ\mathbf{H} \\ \nabla\times\mathbf{H} - a_2\omega^2\left(\nabla\times\mathbf{H}\right)/3 &= j\omega\epsilon_\circ\mathbf{E}, \end{aligned} \tag{8}$$

The form of (8) finally suggests:

$$\begin{aligned} \nabla\times\mathbf{E} + \frac{a_2}{3}\frac{\partial^2}{\partial t^2}\left(\nabla\times\mathbf{E}\right) &= -\mu_\circ\frac{\partial\mathbf{H}}{\partial t} \\ \nabla\times\mathbf{H} + \frac{a_2}{3}\frac{\partial^2}{\partial t^2}\left(\nabla\times\mathbf{H}\right) &= \epsilon_\circ\frac{\partial\mathbf{E}}{\partial t}. \end{aligned} \tag{9}$$

where other rearrangements are possible, as noted in [5].

The result in (9) is the quadratic form of dispersive differential equations [5]. This result is based on the quadratic dispersive velocity model in (2) and on the corresponding Helmholtz equation in (5). The value of a_2 can be obtained from recent gamma-ray measurements where the quantity $\mathcal{E}_p/(\zeta^{1/2}) \approx 5\times10^{18}$ eV [2]. Then, $a_2 = \zeta h^2/(2\pi\mathcal{E}_p)^2 \approx 1.74\times10^{-68}$ s^2 in equation (9). Substituting for a_2 then gives:

$$\begin{aligned} \nabla\times\mathbf{E} + 5.8\times10^{-69}\frac{\partial^2}{\partial t^2}\left(\nabla\times\mathbf{E}\right) &= -\mu_\circ\frac{\partial\mathbf{H}}{\partial t} \\ \nabla\times\mathbf{H} + 5.8\times10^{-69}\frac{\partial^2}{\partial t^2}\left(\nabla\times\mathbf{H}\right) &= \epsilon_\circ\frac{\partial\mathbf{E}}{\partial t}. \end{aligned} \tag{10}$$

The form of the result in (10) is resembles a D-CRLH metamaterial model, as detailed in [5]. The form of the D-CRLH metamaterial model is:

$$\begin{aligned} \nabla\times\mathbf{E} + \epsilon_L\mu\frac{\partial^2}{\partial t^2}\left(\nabla\times\mathbf{E}\right) &= -\mu\frac{\partial\mathbf{H}}{\partial t} \\ \nabla\times\mathbf{H} + \epsilon\mu_L\frac{\partial^2}{\partial t^2}\left(\nabla\times\mathbf{H}\right) &= \epsilon\frac{\partial\mathbf{E}}{\partial t}, \end{aligned} \tag{11}$$

where ϵ_L is defined as left-permittivity in F·m, and μ_L is defined as left-permeability in H·m. The result in (11) is identical to (10) when $\epsilon = \epsilon_\circ$, $\mu = \mu_\circ$, and $a_2/3 = \epsilon_\circ\mu_L = \epsilon_L\mu_\circ \approx 5.8\times10^{-69}$ s^2, giving $\epsilon_L \approx 4.6\times10^{-63}$ F·m and $\mu_L \approx 6.6\times10^{-58}$ H·m.

To show that the solution of (11) has the same phase velocity v_p as (2), first substitute $\mathbf{E} = E_\circ e^{-jkz}e^{j\omega t}\hat{x}$ into (11) to obtain [5]:

$$\begin{aligned} -jk\mathbf{E} - \omega^2\epsilon_L\mu\left(-jk\mathbf{E}\right) &= -j\omega\mu\mathbf{H} \\ -jk\mathbf{H} - \omega^2\epsilon\mu_L\left(-jk\mathbf{H}\right) &= j\omega\epsilon\mathbf{E}\,, \end{aligned}$$

or

$$\begin{aligned} k\left(1-\omega^2\epsilon_L\mu\right)\mathbf{E} &= \omega\mu\mathbf{H} \\ k\left(1-\omega^2\epsilon\mu_L\right)\mathbf{H} &= -\omega\epsilon\mathbf{E}\,. \end{aligned}$$

Substituting the second equation into the first gives:

$$k\left(1-\omega^2\epsilon_L\mu\right)\mathbf{E} = -\omega\mu\frac{\omega\epsilon}{k\left(1-\omega^2\epsilon\mu_L\right)}\mathbf{E}\,,$$

so

$$v_p^2 = \frac{\omega^2}{k^2} = \frac{\left(1-\left(\frac{\omega}{\omega_1}\right)^2\right)\left(1-\left(\frac{\omega}{\omega_2}\right)^2\right)}{\mu\epsilon}\,, \tag{12}$$

where $\omega_1 = 1/\sqrt{\epsilon_L\mu}$ and $\omega_2 = 1/\sqrt{\epsilon\mu_L}$. Since $a_2/3 = \epsilon_\circ\mu_L = \epsilon_L\mu_\circ$, this is further simplified to

$$v_p^2 = \frac{\left(1-a_2\omega^2/3\right)^2}{\mu_\circ\epsilon_\circ} = c^2\left(1-a_2\omega^2/3\right)^2\,, \tag{13}$$

thus returning the original dispersion relation in (2). For low frequencies where $\omega^2 \ll 3/a_2$, (13) gives the normal nearly-constant right-handed phase velocity governed by $v_p^2 \approx c^2$. Taking the positive root, the phase velocity becomes $v_p = \omega/k \approx c$, and the wavenumber becomes $k = \omega/c$. The group velocity is then $v_g = \partial\omega/\partial k = c$. And so, the system (13) is right-handed at low frequency, since v_g and v_p have the same sign [7].

At high frequencies where $\omega^2 \gg 3/a_2$, the result in (13) gives a highly dispersive left-handed velocity set by $v_p^2 \approx \omega^4c^2a_2^2/9$. Taking the negative root, the phase velocity becomes $v_p = -\omega/k \approx -\omega^2ca_2/3$, and the wavenumber becomes $k = -3/(\omega ca_2)$. The group velocity is then $v_g = \partial\omega/\partial k = 3/(k^2ca_2)$. And so, the system (13) is left-handed at high frequency, since v_g and v_p have the opposite sign [7]. Since (10) and (11) have the same form, the resulting phase and group velocities for (10) are plotted in Fig. 1. The group velocity for the proposed model in (10) is plotted as a solid

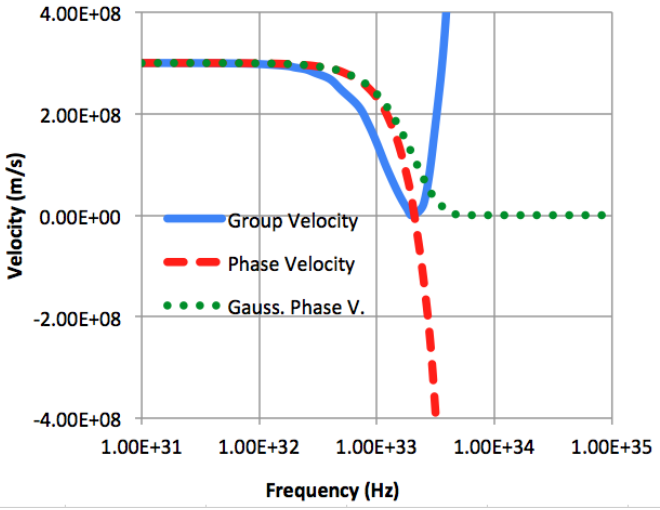

Fig. 1. Plot of phase velocity v_p and group velocity v_g as a function of frequency in Hz. The solid blue curve is the quadratic model group velocity v_g from (2) and (10). The dashed red curve is the quadratic model phase velocity v_p from (2) and (10), using the positive root of the equation for v_p^2 from (13). The dotted green curve shows the Gaussian model phase velocity from (14) and (17) for the same value of a_2, and it closely follows the quadratic model phase velocity at low frequencies. Note that the resonance near 2×10^{33} Hz corresponds to 8.3×10^{9} GeV and is well below the Planck frequency of 2.95×10^{42} Hz, and is well above the 7.5×10^{24} Hz (31 GeV) photon observed in gamma burst GRB 090510 of May of 2009.

blue line in Fig. 1. The phase velocity associated with positive group velocity for (10) is plotted as a dashed red line in Fig. 1, where v_p was taken as the positive or negative root for v_p^2 in (13) that results in a positive group velocity v_g.

III. Empirical Gaussian Dispersion Model

As can be seen in Fig. 1, the model of (10) results in the potential for some unusual phenomena, including superluminal velocities, left-handed propagation, strong dispersion, slow light, and evanescent modes. Such types of unusual phenomena occur when a finite-degree polynomial model is used to model dispersion along the lines of (2), since the highest power of ω in the polynomial will dominate at sufficiently high frequency.

To circumvent some of these unusual effects, a novel Gaussian dispersion model is proposed as an alternative. To arrive at this new model, consider the Taylor series expansion of $e^x = 1+x+x^2/2!+\ldots$ as an approximation of (2):

$$v_p \approx c\left(1 - a_2\omega^2/3\right) \approx c\, e^{-a_2\omega^2/3}\,, \tag{14}$$

where the quadratic dispersion model is now replaced by a Gaussian model. The Gaussian will provide a good approximation to the quadratic for $a_2\omega^2/3 \ll 1$ at low frequencies where $\omega^2 \ll 3/a_2$. One immediate advantage of the Gaussian form of (14) is that the associated phase velocity v_p is now always less than c, thus avoiding the aforementioned superluminal velocity phenomena.

In Fig. 1, the green dotted curve shows the Gaussian dispersive phase velocity from (14). At low frequencies, note that the Gaussian phase velocity of the green dotted curve provides a good approximation to the quadratic polynomial phase velocity of the dashed red curve in Fig. 1. Thus, *the Gaussian model also provides an empirical fit to the measured data*, since it closely matches the low-frequency quadratic model.

Also, note that the group velocity v_g of the Gaussian model (14) is positive, and that $v_g \le c$. To see this, first recall that $v_p = \omega/k \approx c\, e^{-a_2\omega^2/3}$ from (14), so that $k \approx \omega c^{-1}\, e^{a_2\omega^2/3}$. Then, $\partial k/\partial\omega = c^{-1}(1+2\omega^2 a_2/3)e^{a_2\omega^2/3}$, and

$$v_g = \partial\omega/\partial k = c\,\frac{e^{-a_2\omega^2/3}}{1+2\omega^2 a_2/3}\,. \tag{15}$$

Thus, the Gaussian model of (14) and (15) is right-handed for all frequencies, since v_g and v_p have the same sign for all frequencies [7]. In addition, it is straightforward to see that the maximum value of v_g equals c at $\omega = 0$, since the numerator $ce^{-a_2\omega^2/3}$ is a strictly decreasing positive function of ω for $\omega > 0$, and the denominator $1+2\omega^2 a_2/3$ is a strictly increasing positive function of ω for $\omega > 0$.

Using (14), the dispersive form of the Helmholtz equation of (5) would then become:

$$\begin{aligned}\nabla^2\mathbf{E} &= \frac{-\omega^2}{c^2 e^{-2a_2\omega^2/3}}\mathbf{E} \\ &= -\frac{\mu_\circ}{e^{-a_2\omega^2/3}}\,\frac{\epsilon_\circ}{e^{-a_2\omega^2/3}}\,\omega^2\mathbf{E},\end{aligned} \tag{16}$$

and (8) would then become:

$$\begin{aligned}e^{-a_2\omega^2/3}\ \nabla\times\mathbf{E} &= -j\omega\mu_\circ\mathbf{H} \\ e^{-a_2\omega^2/3}\ \nabla\times\mathbf{H} &= j\omega\epsilon_\circ\mathbf{E},\end{aligned} \tag{17}$$

Taking the inverse Fourier transform of (17) directly, results in time convolution on the left side:

$$\begin{aligned}\sqrt{3/(4a_2\pi)}\ e^{-3t^2/(4a_2)} * \nabla\times\mathbf{E} &= -\mu_\circ\frac{\partial\mathbf{H}}{\partial t} \\ \sqrt{3/(4a_2\pi)}\ e^{-3t^2/(4a_2)} * \nabla\times\mathbf{H} &= \epsilon_\circ\frac{\partial\mathbf{E}}{\partial t}\,.\end{aligned} \tag{18}$$

Finally, note that the proposed dispersive differential equations in (8), (10), and (17) revert to the normal form of Maxwell's equations in (4) at low frequencies, with a right-handed electromagnetic wave solution. In essence, the additional terms in equations (8), (10), and (17) behave as dispersive extensions of Maxwell's equations. At extremely high frequencies, the second term on the left side of (8) dominates, and the solution becomes dispersive and left-handed, similar to other dispersive relationships found in metamaterials, optics, and left-handed microwave structures [5]. On the other hand, the proposed Gaussian form in (17) remains right-handed with $|v_p| \le c$ and $|v_g| \le c$ for all frequencies.

IV. Comparisons with Measured Data

Given the Gaussian model of (14) and (17), and given the quadratic model of (2) and (8), the predicted dispersion may now be compared to measured gamma-ray dispersion for several gamma-ray bursts. Since $e^{-a_2\omega^2/3} \approx 1 - a_2\omega^2/3$ for $\omega^2 \ll 3/a_2$, or for $\omega \ll 1.31\times10^{34}$, the numerical results are identical for all practical purposes for photons with energy less

TABLE I
COMPARISON OF MEASURED AND PREDICTED DISPERSIVE TIME DELAYS Δt FOR HIGH ENERGY PHOTONS IN FOUR DIFFERENT GAMMA-RAY BURSTS USING $\mathcal{E}_p/\zeta^{1/2} = 5.0 \times 10^{18}$ AND $a_2 = 1.73 \times 10^{-68}$

Gamma-Ray Burst	Redshift z	Photon Energy (GeV)	Measured Δt (s)	Predicted Δt (s)
GRB 080916C	4.35	13.2	16.5	62.8
GRB 90510	0.90	31.0	0.83	37.5
GRB 090902B	1.82	33.4	82	104.8
GRB 090926A	2.11	19.6	26	45.3

TABLE II
COMPARISON OF MEASURED AND PREDICTED DISPERSIVE TIME DELAYS Δt FOR HIGH ENERGY PHOTONS IN FOUR DIFFERENT GAMMA-RAY BURSTS USING $\mathcal{E}_p/\zeta^{1/2} = 1.4 \times 10^{19}$ AND $a_2 = 2.22 \times 10^{-69}$

Gamma-Ray Burst	Redshift z	Photon Energy (GeV)	Measured Δt (s)	Predicted Δt (s)
GRB 080916C	4.35	13.2	16.5	8.1
GRB 90510	0.90	31.0	0.83	4.9
GRB 090902B	1.82	33.4	82	13.5
GRB 090926A	2.11	19.6	26	5.9

than 31 GeV ($7.5{\times}10^{24}$ Hz). Thus, only one set of comparisons between measured and predicted gamma-ray dispersion time delays is required. It is also apparent by inspection of Fig. 1 that the Gaussian model nearly equals the quadratic model for 31 GeV photons at 7.5×10^{24} Hz.

When computing the predicted time delays, the redshift z of the gamma-ray source must be considered. Since the Gaussian model is well-approvimated by a quadratic at low frequencies, a quadratically-dispersive cosmological computation is used for estimating dispersive time delay. For quadratic dispersion on a cosmological scale, the time delay of GeV photons relative to very low frequency photons may be obtained using [2], [8]:

$$\Delta t \approx \frac{1.5}{H_\circ} \zeta \frac{{\mathcal{E}_\omega}^2}{\mathcal{E}_p^2} \int_0^z \frac{1+\alpha}{\sqrt{\Omega_M (1+\alpha)^3 + \Omega_\Lambda}} \, \partial\alpha \,, \quad (19)$$

where $\mathcal{E}_\omega = h\omega/(2\pi)$ is photon energy in eV, $\mathcal{E}_p = 1.22 \times 10^{28}$ eV, $\zeta = a_2(2\pi\mathcal{E}_p)^2/h^2$, $H_\circ = 2.30 \times 10^{-18}$ s^{-1} is the Hubble constant, z is the redshift of the gamma burst, and $\Omega_M = 0.27$ and $\Omega_\Lambda = 0.73$ are cosmological constants.

Table I provides a comparison of predicted dispersive time delays Δt and measured dispersive time delays Δt, for the same four gamma-ray bursts tabulated by Shao *et al.* [2]. In computing the predicted time delays, the value of $\mathcal{E}_p/\zeta^{1/2} = 5.0{\times}10^{18}$ results in $a_2 = 1.73{\times}10^{-68}$, and was derived by Shao *et al.* using curve-fitting methods. (Note that $\mathcal{E}_p/\zeta^{1/2}$ here is equivalent to $E_{QG,Q}$ in Shao *et al.*) As can be seen in Table I, the proposed models provide better prediction of the long gamma-bursts (durations grater than 2 s) GRB 080916C, GRB 090902B, and GRB 091003A. However, the short gamma-ray burst (durations less than 2 s) of GRB 090510 has a predicted time delay of 37.5 s that is a factor of 45.2 larger than the measured time delay of 0.83 s for the 31 GeV photon. This large variation may not be unexpected, since Shao *et al.* noted that there was over an order of magnitude variation in the measured astronomical data for $\mathcal{E}_p/\zeta^{1/2}$. At present, the body of available gamma-ray data is somewhat limited, especially for gamma sources with high redshift and photons above 10 GeV.

Noting the large variation in measured parameters, Shao *et al.* also provided the average value of $\mathcal{E}_p/\zeta^{1/2} = 1.4 \times 10^{19}$ eV. Using this average value instead of the curve-fit value, Table II provides a second comparison of predicted and measured dispersive time delays using this average value of $\mathcal{E}_p/\zeta^{1/2} = 1.4 \times 10^{19}$ eV and a corresponding new value of $a_2 = 2.22 \times 10^{-69}$ s^2. As can be seen in Table II, the average value of $\mathcal{E}_p/\zeta^{1/2}$ provides better predicted time delay of 4.9 s for the short gamma-ray burst GRB 090510, and all of the predicted time delays fall within an order of magnitude of the measured time delays. Thus, the average value of $\mathcal{E}_p/\zeta^{1/2}$ may serve better for the purpose of estimating dispersive time delay Δt. But again, it is somewhat difficult to draw firm conclusions at this time since the available measured data appears to vary by more than an order of magnitude according to Shao *et al.* [2].

V. CONCLUSION

The dispersion observed in gamma-ray bursts suggests the need for corresponding adjustments to the Helmholtz equation. Although earlier investigators have proposed quadratic dispersion models, these models can exhibit superluminal behavior. The proposed Gaussian dispersion model has the advantage of avoiding superluminal group velocities and phase velocities while still approximating a quadratic polynomial at low frequency. Comparisons of measured dispersion with predicted dispersion show good agreement, within the context of the known order of magnitude variation in currently available measured data for high redshift GeV photons.

REFERENCES

[1] L. Baldini, "The commissioning and first light of the fermi large area telescope," *Nuclear Inst. and Meth. in Physics Res. Sec. A: Accel., Spectr., Det. and Assoc. Equip.*, vol. 604, no. 1-2, pp. 164–167, 2009.

[2] L. Shao, Z. Xiao, and B.-Q. Ma, "Lorentz violation from cosmological objects with very high energy photon emissions," *Astroparticle Physics*, vol. 33, no. 5-6, pp. 312–315, 2010.

[3] G. Amelino-Camelia, J. Ellis, N. E. Mavromatos, D. V. Nanopoulos *et al.*, "Tests of quantum gravity from observations of γ-ray bursts," *Nature*, vol. 393, pp. 763–765, 1998.

[4] A. Abdo, M. Ackermann, M. Ajello, K. Asano *et al.*, "A limit on the variation of the speed of light arising from quantum gravity effects," *Nature*, vol. 462, pp. 331–334, 2009.

[5] T. P. Weldon, R. S. Adams, K. Daneshvar, and R. K. Mulagada, "Metamaterials, gamma-ray bursts, quantum gravity, and the search for the missing half of the maxwell equations," in *IEEE MTT-S Int. Microw. Symp. Dig.*, Jun. 2011.

[6] S. Ramo, J. R. Whinnery, and T. Van Duzer, *Fields and Waves in Communication Eelctronics, 2nd Ed.,*. New York: John Wiley and Sons, 1984.

[7] A. Lai, T. Itoh, and C. Caloz, "Composite right/left-handed transmission line metamaterials," *IEEE Microw. Mag.*, vol. 5, no. 3, pp. 34–50, Sep. 2004.

[8] U. Jacob and T. Piran, "Lorentz-violation-induced arrival delays of cosmological particles," *Journal of Cosmology and Astroparticle Physics*, vol. 2008, no. 01, pp. 31.1–31.4, Jan. 2008.